Journal of Inorganic Biochemistry xxx (2016) xxx–xxx

Contents lists available at ScienceDirect

Journal of Inorganic Biochemistry

journal homepage: www.elsevier.com/locate/jinorgbio

Investigation of the identity of the nucleophile initiating the hydrolysis of phosphate esters catalyzed by dinuclear mimics of metallohydrolases☆

Joshua J. Brown [a], Lawrence R. Gahan [a,*], Anne Schöffler [b], Elizabeth H. Krenske [a], Gerhard Schenk [a]

[a] School of Chemistry and Molecular Biosciences, The University of Queensland, Brisbane 4072, Australia
[b] Institute of Organic Chemistry, Ruprecht-Karls-University Heidelberg, Im Neuenheimer Feld 270, D-69120 Heidelberg, Germany

ARTICLE INFO

Article history:
Received 9 October 2015
Received in revised form 17 January 2016
Accepted 10 February 2016
Available online xxxx

Keywords:
Di-zinc(II) complexes
Nucleophile
Hydrolysis reaction
Phosphodiester
Computational methods

ABSTRACT

di-Zinc(II) complexes of the ligands 2,6-bis((bis(2-methoxyethyl)amino)methyl)-4-methylphenol (HL1), 2,6-bis(bis(hydroxyethyl)aminomethyl)-4-methylphenol (HL2) and 2,6-bis((hydroxyethyl)(methoxyethyl)-aminomethyl)-4-methylphenol (HL3) have been prepared and characterized. The three ligands differ in their donor types, having ether donors (HL1), alkoxido donors (HL2) and both ether and alkoxido donors (HL3). These differences allowed an investigation into the role of the potential nucleophiles in the hydrolysis reaction with the phosphodiester substrate bis(2,4-dinitrophenyl)phosphate (BDNPP). In addition, the di-Mg(II) complex of ligand HL2 was prepared in order to examine the potential for Mg(II) to replace Zn(II) in these biomimetic systems. Kinetically relevant pK_a values for the three di-Zn(II) complexes were determined to be 7.14 and 9.21 for $[Zn_2(L1)(CH_3COO)_2](PF_6)$, 7.90 and 10.21 for $[Zn_2(L2)(CH_3COO)_2](BPh_4)$ and 8.43 and 10.69 for $[Zn_2(L3)(CH_3COO)_2](BPh_4)$. At the respective pH optima the relevant catalytic parameters are $k_{cat} = 5.44(0.11) \times 10^{-5}$ s^{-1} ($K_m = 5.13(0.92)$ mM), $2.60(0.87) \times 10^{-4}$ s^{-1} ($K_m = 5.49(1.51)$ mM) and $1.53(0.27) \times 10^{-4}$ s^{-1} ($K_m = 2.14(0.50)$ mM) for $[Zn_2(L1)(CH_3COO)_2](PF_6)$, $[Zn_2(L2)(CH_3COO)_2](BPh_4)$ or $[Zn_2(L3)(CH_3COO)_2](BPh_4)$, respectively. The di-Mg(II) complex was found to be unreactive in the hydrolysis reaction with BDNPP under the conditions employed. Computational methods using the $[Zn_2(L2)(CH_3COO)_2](BPh_4)$ complex were used to discriminate between different possible mechanistic pathways. The DFT calculations indicate that an alkoxido-mediated pathway in the complexes formed with ligands L2 or L3 is unlikely, because it induces significant distortion of the $Zn_2(L)$ unit; a direct attack by a coordinated hydroxide is preferred in each of the three systems studied here. The calculations also revealed the important role of ligand structural rigidity.

1. Introduction

We and others, have explored extensively the functional roles that model complexes can play in reproducing the electronic, structural and reactivity characteristics of organophosphate-hydrolyzing metalloenzyme systems [1–26]. One of the prominent issues targeted in these studies is the identity of the nucleophilic agent(s) in the models and in the corresponding metalloenzymes [27]. It is generally accepted that in the key chemical step in hydrolytic enzymes a hydroxide acts as the pertinent nucleophile [27]. This hydroxide may be coordinated directly to a metal ion in the active site, or be located in the second coordination sphere, activated through hydrogen bonding interactions with amino acid side chains and/or water molecules lining the active site of the enzyme [27–29]. Exogenous moieties (*e.g.* serine residues) have also been implicated as potential nucleophiles in enzymes such as alkaline phosphatases [27]. Among the various described model systems there are examples of both complexes that use a metal ion-coordinated hydroxide as nucleophile, and those that use an alkoxide moiety for this role [1,30]. In the case of a number of zinc(II) complexes it has been proposed that a coordinated alcohol group is a stronger nucleophile than a coordinated hydroxide [1,30,31]; in addition, it has been suggested that the coordinated alcohol is deprotonated at or below the same pH as a coordinated water molecule [31]. However, it should be pointed out that in metallohydrolases, enzymes and corresponding model complexes, the unambiguous identification of relevant nucleophiles and hence the elucidation of the mechanistic pathway is difficult [25,30].

Here, in order to address the issue of identifying relevant nucleophiles, we describe the synthesis and characterization of the di-zinc(II) complexes of three closely related ligands, 2,6-bis((bis(2-methoxyethyl)amino)methyl)-4-methylphenol (HL1), 2,6-bis(bis(hydroxyethyl)aminomethyl)-4-methylphenol (HL2), and 2,6-bis((hydroxyethyl)(methoxyethyl)-aminomethyl)-4-methylphenol (HL3) (Chart 1) [20,32–40]. These ligands provide ether donor (HL1), or alkoxido donor ligands (HL2), or an asymmetric combination (HL3) with both ether and alkoxido ligands. The catalytic potential of these complexes has been explored using the phosphodiester substrate

☆ In memory of Professor Graeme Hanson and his contributions to bioinorganic chemistry and electron paramagnetic resonance.

* Corresponding author.
E-mail address: gahan@uq.edu.au (L.R. Gahan).

http://dx.doi.org/10.1016/j.jinorgbio.2016.02.008
0162-0134/

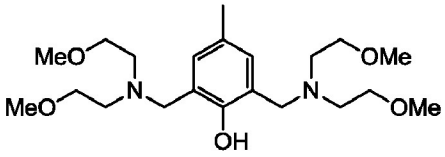

2,6-bis((bis(2-methoxyethyl)amino)methyl)-4-methylphenol (HL1)

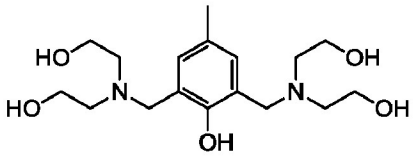

2,6-bis(bis(hydroxyethyl)aminomethyl)-4-methylphenol (HL2)

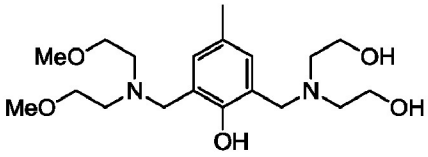

2,6-bis((hydroxyethyl)(methoxyethyl)-aminomethyl)-4-methylphenol (HL3)

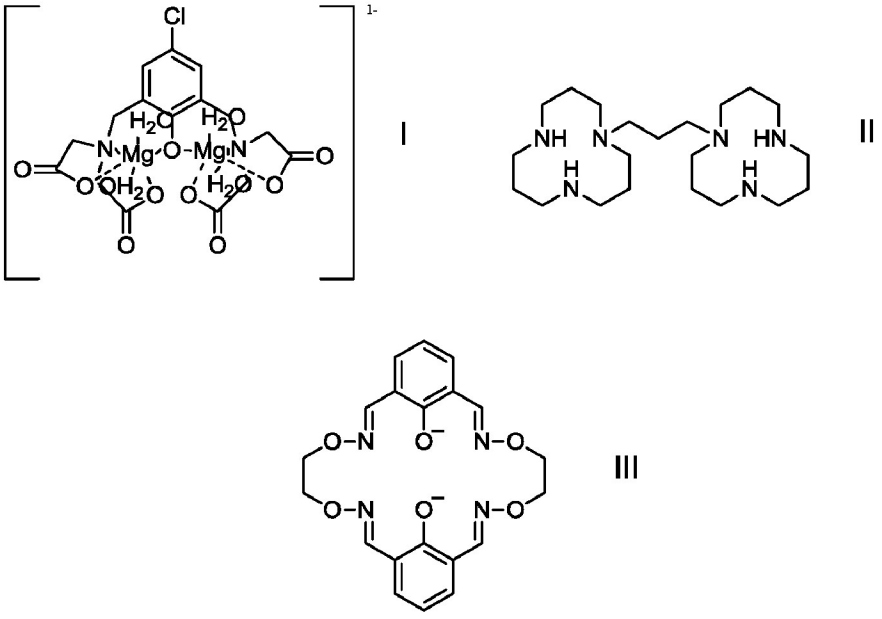

Chart 1. Ligands discussed in this work.

bis(2,4-dinitrophenyl)phosphate (BDNPP). In addition, we have employed computational methods in an attempt to discriminate between different mechanistic pathways possible for these systems. As part of this study the di-Mg(II) complex of ligand HL2 has also been prepared with a view to examining a previous suggestion that Mg(II) is able to replace Zn(II) in these hydrolytic enzyme model systems [41–43].

2. Experimental

2.1. General methods and materials

Elemental microanalyses (C, H, N, S) were performed by the Micro-analytical service at the School of Chemistry and Molecular Biosciences, the University of Queensland. UV–vis spectroscopy was recorded with an Agilent 8453 UV–visible Spectrophotometer, IR spectra were recorded with a Perkin-Elmer Frontier FT-IR/NIR spectrometer SPECTRUM 400 (mode: MIR) with a Smiths DuraSamplIR II ATR diamond window. The software used for data processing was Perkin Elmer Spectrum version 10.03.09. ^{1}H NMR spectra were recorded at room temperature with a 300 MHz Bruker AV 300/400 spectrometer. The abbreviations s = singlet, d = doublet, t = triplet, m = multiplet have been employed. ^{13}C NMR spectra were recorded at room temperature with a 100 MHz Bruker AV 400 spectrometer. Chemical shifts are reported relative to d^{4}-MeOD (δ_C = 49.0(7)). The software used for data processing was TOPSPIN 3.0 from Bruker. For column chromatography silica gel (SiO_2, grain size 0.04–0.06 nm) produced by Scharlan was used. Solvent mixtures of methanol and ethyl acetate mobile phases were used.

Please cite this article as: J.J. Brown, et al., Investigation of the identity of the nucleophile initiating the hydrolysis of phosphate esters catalyzed by dinuclear mimics of me..., J. Inorg. Biochem. (2016), http://dx.doi.org/10.1016/j.jinorgbio.2016.02.008

2.2. X-ray crystallography

Crystallographic data for the complexes were collected unless otherwise stated at 293(2) K with an Oxford Diffraction Gemini Ultra dual source (Mo and Cu) CCD diffractometer with Mo ($\lambda_{K\alpha} = 0.71073$ Å) or Cu ($\lambda_{K\alpha} = 1.5418$ Å) radiation. The structures were solved by direct methods (SIR-92) and refined (SHELXL 97) by full matrix least square methods based on F^2 [44]. These programs were accessed through the WINGX 1.70.01 crystallographic collective package [45]. All non-hydrogen atoms were refined anisotropically unless they were disordered. Hydrogen atoms were fixed geometrically and were not refined. X-ray data of the published structures were deposited with the Cambridge Crystallographic Data Centre CCDC1429598-1,429,601. Crystal data are given in Table 1 and selected bond distances and bond angles in Table 2.

2.3. Syntheses

The 2,6-bis(chloromethyl)-4-methylphenol precursor was prepared as previously described [46]. The preparation of ligand HL1, and the characterization of a number of complexes of this ligand, has been reported previously [32–40].

2.3.1. 2,6-bis((bis(2-methoxyethyl)amino)methyl)-4-methylphenol (HL1)

A solution of bis(2-methoxyethyl)amine (2.66 g, 20.0 mmol) in triethylamine (2.77 mL, 20.0 mmol) and tetrahydrofuran (10 mL) was prepared and cooled to 0 °C. A solution of 2,6-bis(chloromethyl)-4-methylphenol (2.05 g, 10.0 mmol) in dichloromethane (8 mL) was added drop wise. The mixture was stirred at room temperature for 48 h and then filtered to remove the colorless precipitate of triethylamine hydrochloride. Removal of the solvents left a yellow oil which was purified by column chromatography (ethyl acetate/methanol 4:1) (yield 1.52 g, 37%). ^{1}H NMR (300.13 MHz, $CDCl_3$): δ = 7.10 (s, 2H), 4.10 (s, 4H), 3.67 (s, 8H), 3.31 (s, 12H), 3.07 (s, 8H), 2.22 (s, 3H) ppm.

2.3.2. 2,6-bis(bis(hydroxyethyl)aminomethyl)-4-methylphenol (HL2)

2,6-chloromethyl-4-methylphenol (2.06 g, 10.0 mmol) in dichloromethane (9 mL) was added slowly to a solution of dihydroxyethylamine (1.9 mL, 19.8 mmol), triethylamine (2.8 mL) and tetrahydrofuran (10 mL) at 0 °C. The resulting crude oil was purified in methanol with column chromatography (yield, 1.58 g, 46.1%). ^{1}H NMR (300.13 MHz, D_2O): δ = 6.92 (s, 2H), 3.76 (s, 4H), 3.64 (t, $^3J_{H,H}$ = 5.7 Hz, 8H), 3.24 (s, MeOH), 2.73 (t, $^3J_{H,H}$ = 6.0 Hz, 8H), 2.12 (s, 3H) ppm.

2.3.3. 2,6-bis(bis(methoxyethyl)-aminomethyl)-4-methylphenol (HL1) and 2,6-bis((hydroxyethyl)(methoxyethyl)-aminomethyl)-4-methylphenol (HL3)

2,6-chloromethyl-4-methylphenol (3.08 g, 15.0 mmol) in dichloromethane (12 mL) was added slowly to a solution of dihydroxyethylamine (2.6 mL 27.0 mmol) and dimethoxyethylamine (3.95 mL 27.0 mmol), triethylamine (3.75 mL) and tetrahydrofuran (13.5 mL) at 0 °C. The resulting crude oil was purified in methanol with three rounds of column chromatography, each ligand isolated separately (HL1 yield 0.18 g, 3.35%; HL2 yield 0.17 g, 3.67%; HL3 yield 0.42 g, 7.55%). HL3: ^{1}H NMR (300.13 MHz, D_2O): δ = 6.93–6.91 (d, $^2J_{H,H}$ = 6.0 Hz, 2H), 3.71 (s, 4H), 3.63 (t, $^3J_{H,H}$ = 6.0 Hz, 4H), 3.50 (t, $^3J_{H,H}$ = 5.7 Hz, 4H), 3.25 (s, MeOH), 3.22 (s, 6H), 2.72–2.70 (m, 5.4 Hz–5.7 Hz, 8H), 2.13 (s, 3H).

2.4. Syntheses of the metal complexes

2.4.1. $[Zn_2(L1)(CH_3COO)_2](PF_6)$

2,6-bis((bis(2-methoxyethyl)amino)methyl)-4-methylphenol **2** (0.10 g, 0.25 mmol) was dissolved in methanol (5 mL) and a solution of zinc acetate dihydrate (0.11 g, 0.50 mmol) in methanol (5 mL) was added drop wise. The colorless solution was refluxed (70 °C) for 0.5 h and then cooled to room temperature. Sodium hexafluorophosphate (0.11 g, 0.60 mmol) was added. The mixture was filtered to remove the excess sodium hexafluorophosphate and the solution was left in a beaker so that the solvent evaporated slowly. Colorless crystals were obtained after 7 days (yield 188 mg, 95%). ^{1}H NMR (300.13 MHz, MeOD): δ = 7.00 (s, 2H), 3.82 (s, 4H), 3.50 (broad s, 4H), 3.36 (s, 12H), 3.07 (broad s, 8H), 2.91 (m, 4H), 2.23 (s, 3H), 2.01 (s, 6H, CH_3COO^-) ppm. ^{13}C NMR (100.62 MHz, MeOD): δ = 177.6 ($CH_3\underline{C}OO^-$), 161.4, 133.2, 127.7, 125.0, 68.9, 62.7, 59.7, 24.4, 20.4 ppm. ESI-MS (methanol) found: m/z = 645.1 $[C_{25}H_{43}N_2O_9Zn_2]^+$, 617.1 $[C_{23}H_{39}N_2O_9Zn_2]^+$, 589.2 $[C_{22}H_{39}N_2O_8Zn_2]^+$. IR ν = 2937 (w, br), 1599 (m), 1481 (w), 1428 (m), 1327 (w), 1278 (w), 1099 (m), 1030 (w), 1003 (w), 826 (s), 665 (m),

Table 1
Crystal data.

	$[Zn_2(L1)(CH_3COO)_2]PF_6$	$[Zn_2(L2)(CH_3COO)_2]BPh_4.CH_3CN$	$[Zn_2(L3)(CH_3COO)_2]BPh_4.2CH_3OH$	$[Mg_2(L1)(CH_3COO)_2]BPh_4$
Empirical formula	$C_{25}H_{43}F_6N_2O_9PZn_2$	$C_{47}H_{58}BN_3O_9Zn_2$	$C_{49}H_{67}BN_2O_{11}Zn_2$	$C_{46}H_{59}BMg_2N_2O_{10.5}$
Formula weight	791.32	950.51	1001.6	867.38
Wavelength (Å)	1.54180	1.54180	1.54180	1.54180
Crystal system	Triclinic	Monoclinic	Monoclinic	Monoclinic
Space group	P-1	$P2_1/n$	C2/c	$P2_1/c$
Crystal size (mm)	0.3 × 0.05 × 0.05	0.5 × 0.5 × 0.5	0.4 × 0.4 × 0.3	0.5 × 0.5 × 0.5
T (K)	190(2)	190(2)	190(2)	190(2)
a (Å)	10.6176(6)	15.0013(5)	28.7875(9)	29.581(2)
b (Å)	12.3509(6)	13.4784(4)	10.8171(3)	13.6638(4)
c (Å)	12.6678(6)	23.7110(10)	31.8882(10)	25.722(2)
α (°)	85.694(4)			
β (°)	86.610(4)	96.725(3)	91.280(3)	115.559(7)
γ (°)	85.979(4)			
Vol (Å^3)	1650.03(15)	4761.2(3)	9927.4(5)	9379.2(10)
Z	2	4	8	8
μ (mm^{-1})	3.007	1.692	1.673	0.936
F (000)	816	1992	4224	3696
ρ (mg/m^3)	1.593	1.326	1.34	1.229
Ind. Reflns	5232	7557	7826	14,711
θ range (°)	3.50–62.50	3.78–62.43	4.09–62.47	3.31–62.45
GOOF on F^2	1.026	1.046	1.051	1.09
Final R indices[I > 2σ(i)]	R1 = .0350	R1 = .0525	R1 = .0362	R1 = .1013
	wR2 = .0853	wR2 = .1485	wR2 = .0922	wR2 = .2569
R indices (all data)	R1 = .0424	R1 = .0599	R1 = .0406	R1 = .1141
	wR2 = .0911	wR2 = .1591	wR2 = .0988	wR2 = .2649

Please cite this article as: J.J. Brown, et al., Investigation of the identity of the nucleophile initiating the hydrolysis of phosphate esters catalyzed by dinuclear mimics of me..., J. Inorg. Biochem. (2016), http://dx.doi.org/10.1016/j.jinorgbio.2016.02.008

Table 2
Selected bond lengths (Å) and angles (°).

M = Zn(II) or Mg(II)	$[Zn_2(L1)(CH_3COO)_2]PF_6$	$[Zn_2(L2)(CH_3COO)_2]BPh_4 \cdot CH_3CN$	$[Zn_2(L3)(CH_3COO)_2]BPh_4 \cdot 2CH_3OH$	$[Mg_2(L1)(CH_3COO)_2]BPh_4$
M(1)-O(1)	2.0119(18)	2.005(2)	1.9982(15)	2.017(4)
M(1)-O(2)	2.1692(19)	2.242(3)	2.1843(16)	2.138(4)
M(1)-O(3)		2.096(2)	2.3747(16)	2.085(5)
M(1)-O(6)	1.9600(19)	2.088(2)	1.9897(17)	2.023(4)
M(1)-N(1)	2.127(2)	2.163(3)	2.1166(19)	2.218(5)
M(2)-N(2)	2.142(2)	2.145(3)	2.1473(19)	2.198(5)
M(2)-O(1)	2.0216(18)	1.990(2)	2.0475(15)	2.013(4)
M(2)-O(4)		2.224(3)	2.1603(17)	2.133(4)
M(2)-O(5)	2.166(2)	2.139(3)	2.2703(19)	2.085(5)
M(2)-O(7)	2.053(2)	2.053(3)	2.1463(17)	2.070(5)
M(1)···M(1)	3.270	3.320	3.282	3.366
O(1)-M(1)-O(2)	171.07(8)	163.77(11)	171.88(7)	165.02(19)
O(1)-M(1)-O(3)		96.68(11)	93.47(6)	95.05(19)
O(1)-M(1)-N(1)	92.36(8)	91.50(10)	93.33(7)	90.19(17)
O(2)-M(1)-O(3)		93.51(12)	89.49(6)	92.75(19)
O(3)-M(1)-N(1)		77.60(10)	75.95(7)	77.20(18)
O(2)-M(1)-N(1)	78.85(9)	78.37(11)	80.05(7)	79.08(17)
O(4)-M(2)-N(2)		80.05(11)	76.78(7)	78.40(18)
O(4)-M(2)-O(5)	85.29(9)	87.18(12)	90.30(8)	92.9(2)
O(1)-M(2)-O(4)		169.48(11)	164.45(7)	165.1(2)
O(1)-M(2)-O(5)	167.93(8)	98.22(11)	94.67(7)	94.91(19)
O(1)-M(2)-N(2)	91.14(8)	92.21(10)	89.90(7)	91.00(18)
O(5)-M(2)-N(2)		77.87(11)	77.51(7)	77.04(19)
M(1)-O(1)-M(2)	108.34(8)	112.43(11)	108.40(7)	113.33(19)

621 (w), 555 (s) cm^{-1}. Anal calc. for $C_{25}H_{43}N_2O_9Zn_2PF_6$ $3H_2O$: C 35.52, H 5.84, N 3.31; found: C 35.83, H 5.34, N 3.21%.

2.4.2. $[Zn_2(L2)(CH_3COO)_2](BPh_4)$

2,6-bis((bis(2-Hydroxyethyl)amino)methyl)-4-methylphenol (0.17 g, 0.5 mmol) was dissolved in methanol (3 mL) and a solution of zinc acetate dihydrate (0.22 g, 1.0 mmol) in methanol (3 mL) was added. The colorless solution was refluxed (65 °C) for 0.75 h and then cooled to room temperature. Sodium tetraphenylborate (0.205 g, 0.60 mmol) was added, the mixture filtered and the solution was left in a beaker so that the solvent evaporated slowly. Colorless crystals were obtained after 2–3 days (yield, 340 mg, 79%). ^{1}H NMR (300.13 MHz, MeOD): [$-BPh_4$ Counterion] δ = 7.30 (broad s, 8H), 6.98 (t, $^3J_{H,H}$ = 7.5 Hz, 8H), 6.84 (t, $^3J_{H,H}$ = 7.2 Hz, 4H) ppm. [Complex] δ = 6.94 (s, 2H), 3.82 (broad s, 4H), 3.62 (broad s, 4H), 3.37 (broad s, 4H), 2.96 (broad s, 4H), 2.74 (broad s, 4H), 2.22 (s, 3H), 1.98 (s, $C\underline{H}_3COO^-$) ppm. ^{13}C NMR (100.62 MHz, MeOD): δ = 178.6 ($CH_3\underline{C}OO^-$), 135.9 ($-BPh_4$), 130.7, 125.7, 124.9 ($-BPh_4$), 123.9, 121.3 ($-BPh_4$), 60.1, 56.6, 22.6 ($\underline{C}H_3COO^-$), 18.9 ppm. IR ν = 3493(m), ~3250(w, broad), 3058(m), 1609 (s), 1578 (m), 1475(w), 1427(s), 1308(w), 1284(w), 1032(M), 889(m), 731(m), 710(s), 620(s) cm^{-1}. Anal calc. for $C_{21}H_{35}N_2O_9Zn_2BPh_4$: C 59.42, H 6.09, N 3.08; found: C 59.42, H 6.12, N 3.08%.

2.4.3. $[Zn_2(L3)(CH_3COO)_2](BPh_4)$

The complex was prepared following a similar procedure as described for complex with ligand HL2. Colorless crystals were obtained with tetraphenylborate anion after 2–3 days but were maintained in the mother liquor prior to collection of X-ray diffraction data (yield, 204 mg 43%). ^{1}H NMR (300.13 MHz, MeOD): δ = [BPh_4 Counterion] δ = 7.25 (broad s, 8H), 6.31 (t, $^3J_{H,H}$ = 7.2 Hz, 8H), 6.80 (t, $^3J_{H,H}$ = 7.2 Hz, 4H) ppm. [Complex] δ = 3.79 (broad s, 4H), 3.57 (broad s, 4H), 3.46 (broad s, 4H), 3.32 (s, 6H), 3.05 (broad s, 4H), 2.75 (broad s, 4H), 2.19 (s, 3H), 1.96 (s, 6H, $C\underline{H}_3COO^-$) ppm. ^{13}C NMR (100.62 MHz, MeOD): δ = 179.0 ($CH_3\underline{C}OO^-$), 136.0 ($-BPh_4$), 131.7, 125.7, 124.9 ($-BPh_4$), 123.6, 121.2($-BPh_4$), 58.0, 22.8 ($\underline{C}H_3COO^-$) ppm. IR ν = ~3300(w, broad), 3055(m), 1578(s), 1478(m), 1423(s), 1327(m), 1273(m), 1098(m), 1088(m), 849(w), 732(s), 704(s), 620(s) cm^{-1}. Anal calc. for $C_{23}H_{39}N_2O_9Zn_2BPh_4$.MeOH: C 59.46, H 6.55, N 2.89; found: C 59.35, H 6.44, N 2.76%.

2.4.4. $[Mg_2(L2)(CH_3COO)_2](BPh_4)$

The complex was prepared following a similar procedure as described for complex with ligand HL2 except magnesium acetate tetrahydrate (0.22 g, 1.0 mmol) was employed. Colorless crystals were obtained after 2–3 days and were left in solution before X-ray diffraction data collection (yield, 290 mg, 70%). ^{1}H NMR (300.13 MHz, MeOD): [$-BPh_4$ Counterion] δ = 7.28 (broad s, 8H), 6.96 (t, $^3J_{H,H}$ = 7.5 Hz, 8H), 6.82 (t, $^3J_{H,H}$ = 7.2 Hz, 4H) ppm. [Complex] 6.90 (s, 2H), 3.91 (s, 4H), 3.70 (t, $^3J_{H,H}$ = 5.4 Hz, 8H), 2.83 (t, $^3J_{H,H}$ = 5.4 Hz, 8H), 2.29 (s, 3H), 1.92 (s, 6H). ^{13}C NMR (100.62 MHz, MeOD): δ = 134.2 ($-BPh_4$), 123.2($-BPh_4$), 119.6 ($-BPh_4$), 55.4, 54.5 ppm. IR ν = ~3240 (w, broad), 3055(m), 1579(s), 1478(m), 1424(s), 1324(m), 1273(m), 1084(s), 847(m), 806(w), 733(s), 704(s), 611(s) cm^{-1}. Anal calc. for ($C_{21}H_{35}N_2O_9Mg_2BPh_4$: C 65.33, H 6.70, N 3.39; found: C 65.67, H 6.72, N 3.42%.

2.4.5. Attempted synthesis of $[Mg_2(L1)(CH_3COO)_2](PF_6)$

2,6-bis((bis(2-Methoxyethyl)amino)methyl)-4-methylphenol (0.11 g, 0.25 mmol) was dissolved in methanol (5 mL) and a solution of magnesium acetate tetrahydrate (0.11 g, 0.50 mmol) in methanol (5 mL) was added drop wise. The colorless solution was refluxed (70 °C) for 0.5 h and then cooled to room temperature. 2.50 eq sodium hexafluorophosphate (0.11 g, 0.60 mmol) were added subsequently. The mixture was filtered to remove the excess sodium hexafluorophosphate and the solution was left in a beaker. Evaporation of the solvent left a colorless oil (54.1 mg, 31%). All attempts to crystallize the complex from a range of solvents were unsuccessful.

ESI − MS (methanol) found : m/z
= 563.3 $[C_{25}H_{43}N_2O_9Mg_2]^+$, 535.3 $[C_{23}H_{39}N_2O_9Mg_2]^+$.

2.5. Phosphatase activity measurements

Kinetic studies of the phosphatase-like activity of the complexes towards the substrate BDNPP were carried out by monitoring the formation of 2,4-dinitrophenolate (DNP) anion at 400 nm. A Varian Cary50 Bio UV/Visible spectrophotometer was employed with 10 mm quartz cuvettes and a Peltier temperature controller to maintain a temperature of 298 K. Measurements were taken using a 50:50 buffer/acetonitrile solution, 40 μM complex and 5 mM BDNPP in

Please cite this article as: J.J. Brown, et al., Investigation of the identity of the nucleophile initiating the hydrolysis of phosphate esters catalyzed by dinuclear mimics of me..., J. Inorg. Biochem. (2016), http://dx.doi.org/10.1016/j.jinorgbio.2016.02.008

acetonitrile. The aqueous buffer consisted of 50 mM MES (2-(N-morpholino)ethanesulfonic acid) (pH 5.50–6.70), HEPES (4-(2-hydroxyethyl)-1-piperazineethanesulfonic acid) (pH 7.00–8.50), CHES (2-(N-cyclohexylamino)ethane sulfonic acid) (pH 9.00–10.00) and CAPS (*N*-cyclohexyl-3-aminopropanesulfonic acid) (pH 10.5–11) at constant ionic strength using 250 mM $LiClO_4$. The pH was adjusted using NaOH to give buffers ranging from pH 5.0 to 10.5. These were then treated with Chelex for 24 h and filtered through a 0.45 μm Millex syringe-driven filter. For the kinetic measurements the complex and buffer were mixed and left for 1 min before the addition of the substrate; after a short period for equilibration in the reaction chamber the initial rates were determined over a period of 3 min. Assays were carried out in 50:50 MeCN:buffer, with substrate and complex initially dissolved in MeCN. The pH values reported are those of the aqueous component; it should however be noted that the pH of a solution of the buffer was the same within error as a 1:1 mixture of buffer and acetonitrile [47,48]. Assays performed to investigate the effect of pH (over a pH range of 5.5–11.0) on the hydrolytic properties of the complexes contained 250 μM of the Zn(II) complexes and 750 μM of the Mg(II) complex with 5 mM of BDNPP; no buffer effects were detected. Assays to assess the effect of the substrate concentration used the same complex concentrations with 1–10 mM in BDNPP. Background assays for autohydrolysis were subtracted from the data. The change in absorbance produced by the hydrolysis of BDNPP by free Zn(II) (from $Zn(CH_3COO)_2{\cdot}2H_2O$), using similar concentrations as with the complexes, did not vary significantly from the measured autohydrolysis rates. All data were fitted by non-linear least square regression analysis.

2.6. Computational modeling

Density functional theory (DFT) calculations were performed in Gaussian 09 [49]. Geometry optimizations employed the B3LYP functional [50–53] and a mixed basis set consisting of LANL2DZ on Zn and 6-31G(d) on other atoms. Harmonic vibrational frequency calculations were used to identify whether stationary points were local minima (zero imaginary vibrational frequencies) or transition states (one imaginary frequency) and to obtain zero-point energy and thermochemical corrections. Solvation energies in water were computed with the SMD implicit solvent model [54] using the same functional and basis set. Single-point energies were then calculated with the M06 functional [55] and a mixed basis set consisting of LANL2DZ on Zn and 6-31G(d,p) on other atoms. Gibbs free energy in solution was calculated by adding the B3LYP zero-point energy, thermochemical corrections and solvation energy to the M06 potential energy. A standard state of 298.15 K and 1 mol/L was used. Certain transition states for P–O bond formation or P–O bond cleavage could not be located by direct optimization to a first-order saddle point. In these cases the procedure for identification of the transition state involved stretching the relevant P–O bond of the phosphorane intermediate in 0.1 Å increments and locating the maximum in ΔG(B3LYP) along the bond-stretching coordinate.

3. Results and discussion

3.1. Syntheses

The ligands described were prepared by the reaction between 2,6-bis(chloromethyl)-4-methylphenol precursor and either bis(2-methoxyethyl)amine, bis(2-hydroxyethyl)amine, or both, the synthetic approach to HL3 utilizing a statistical reaction resulted in HL1, HL2 and HL3 which were separated through column chromatography. The metal complexes were prepared by the reaction of the appropriate ligands with zinc(II) acetate resulting in complexes $[Zn_2(L1)(CH_3COO)_2](PF_6)$, $[Zn_2(L2)(CH_3COO)_2](BPh_4)$ and $[Zn_2(L3)(CH_3COO)_2](BPh_4)$, or the reaction with magnesium(II) acetate to produce $[Mg_2(L2)(CH_3COO)_2](BPh_4)$; attempts to prepare the $[Mg_2(L1)(CH_3COO)_2](PF_6)$ complex resulted in an oil which was not able to be obtained in solid form. However, the mass spectrum in methanol suggested the presence of the desired compound. The crystals of the zinc complexes with HL2 and HL3 as well as the magnesium complex were found to desiccate upon separation from the mother liquor, and were therefore kept in solution prior to structural analysis.

The nomenclature employed for these types of ligands (HL1, HL2 and HL3, Chart 1) follows that described previously [48]. The nomenclature denotes the number of labile protons upon complexation; there are a number of deprotonations possible — from the phenolic –OH and from the alcohol pendant arms of the ligands. The analyses of the complexes suggest that in all cases a single anionic entity is present (PF_6^- or BPh_4^-) and that a single deprotonation of the ligand has occurred on complexation. Therefore, designation of the ligand as L1, L2 and L3 implies a single deprotonation and a monoanionic ligand.

3.2. X-ray structures

The X-ray crystal structures of the four complexes all show the presence of a complex cation composed of the respective ligand, and two metal ions triply linked by the deprotonated phenol moiety from the ligand and by two bridging acetate groups, with either tetraphenylborate or hexafluorophosphate as the uncoordinated anion. Selected crystallographic data are shown in Table 1, selected bond lengths and angles are displayed in Table 2. ORTEP plots of the four complex cations are shown in Fig. 1(a)–(d).

For the complexes $[Zn_2(L2)(CH_3COO)_2](BPh_4)$, $[Zn_2(L3)(CH_3COO)_2](BPh_4)$ and $[Mg_2(L2)(CH_3COO)_2](BPh_4)$ each six coordinate metal ion environment is composed of a NO_5 chromophore containing a tertiary amine, two alcohol and/or ether-O donors, and two oxygens from the bridging acetates. The six-coordinate geometry is completed by the bridging oxygen from the phenoxide in each case. The Zn–O and Zn–N distances are typical of those reported for this type of complex [1,23,30,35,56]. The structure of the zinc(II) complex with ligand HL1 has been reported previously as the tetraphenylborate salt, $[Zn_2(L1)(CH_3COO)_2]BPh_4$ [35]; in our case the PF_6^- salt, $[Zn_2(L1)(CH_3COO)_2](PF_6)$, was isolated. Both structures exhibit two short Zn(II)–O–CH_3 bonds (2.166 and 2.1669 Å, PF_6^-; 2.214(5) and 2.197(3) Å, BPh_4^-) and two are considerably longer (2.523 and 2.528 Å, PF_6^-;2.362(4) and 2.440(3) Å, BPh_4^-) [35]. This has also been observed previously for similar zinc complexes [1]. The metal–metal distances range from 3.270 Å to 3.366 Å, the longest being that for the di-Mg(II) complex.

There are numerous reports of di-Mg(II) complexes in the literature with many examples of phenoxo-bridged macrocycles [57–72]. Of relevance to this work is the reported structure of the complex hemi[hexaaquamagnesium(II)](μ-2,6-bis[(bis(carboxylatomethyl)amino)methyl]-4-chlorophenolato)bis[diaquamagnesium(II)] decahydrate (Chart 1, I) [70], which has Mg–N distances of 2.210(2) Å and 2.201(2) Å compared to 2.197(5) Å and 2.218(5) Å in $[Mg_2(L2)(CH_3COO)_2](BPh_4)$. Furthermore, for $[Mg_2(L2)(CH_3COO)_2](BPh_4)$ Mg-μ-O(phenoxide) 2.016(4) Å and 2.013(4) Å, Mg…Mg 3.366 Å and Mg–O–Mg 113.37(19)° whilst for the previously reported structure [70], Mg-μ-O(phenoxide) 2.062(2) Å and 2.072(2) Å, Mg…Mg 3.787(1) Å, and Mg–O–Mg 132.72(9)°.

3.3. Phosphatase-like activity

Phosphatase-like activities of the zinc complexes $[Zn_2(L1)(CH_3COO)_2](PF_6)$, $[Zn_2(L2)(CH_3COO)_2](BPh_4)$, $[Zn_2(L3)(CH_3COO)_2](BPh_4)$ were measured using the activated substrate BDNPP. Based on a series of previous studies [30,73–80] the underlying assumption of our approach is that the two metal ion-bridging acetate groups dissociate in aqueous environment, thus providing binding sites for the substrate and water molecules from the solvent. While other scenarios are, in

Please cite this article as: J.J. Brown, et al., Investigation of the identity of the nucleophile initiating the hydrolysis of phosphate esters catalyzed by dinuclear mimics of me..., J. Inorg. Biochem. (2016), http://dx.doi.org/10.1016/j.jinorgbio.2016.02.008

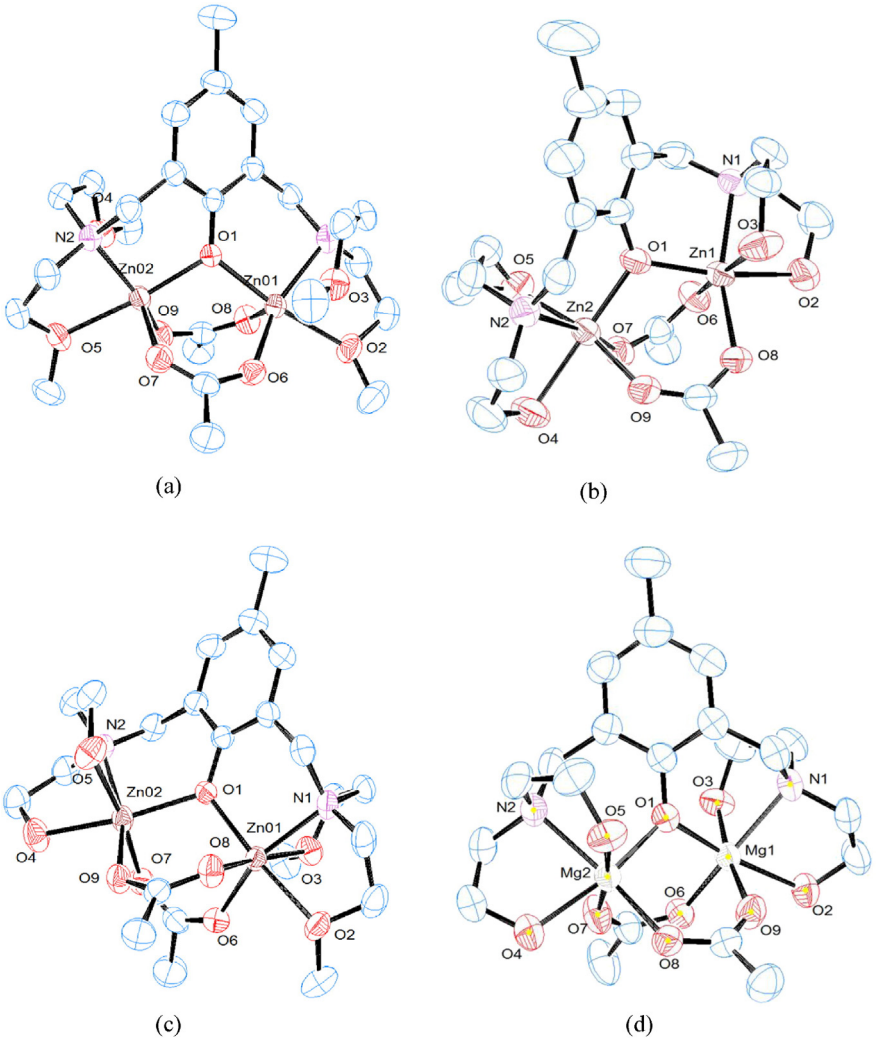

Fig. 1. ORTEP plot of (a) $[Zn_2(L1)(CH_3COO)_2]^+$; (b) $[Zn_2(L2)(CH_3COO)_2]^+$ (disorder is present in one chelate ring); (c) $[Zn_2(L3)(CH_3COO)_2]^+$; (d) $[Mg_2(L2)(CH_3COO)_2]^+$. Hydrogen atoms, counter ions and labels of non-coordinating atoms have been omitted for clarity.

principle, possible (*e.g.* partial dissociation of one or both acetate groups) there is currently no evidence to support these alternatives. For each complex the dependence of the reaction rate on pH was determined in the range between pH 5 to 10.5. The pH-rate profiles for each of the three Zn complexes follow a bell-shaped curve but their pH maxima differ (Fig. 2a). $[Zn_2(L1)(CH_3COO)_2](PF_6)$ exhibits a rate maximum at pH 8 whereas $[Zn_2(L2)(CH_3COO)_2](BPh_4)$ and $[Zn_2(L3)(CH_3COO)_2](BPh_4)$ display maxima at pH 9 and 9.5, respectively. The pH profiles were fitted using Eq. (1) [81]:-

$$v_0 = \frac{v_{max}}{\left(1 + \frac{[H^+]}{K_{a1}} + \frac{K_{a2}}{[H^+]}\right)} \quad (1)$$

where v_0 is the rate of formation of DNP ($M\,s^{-1}$) and v_{max} is the maximal (pH independent) rate. From the fitted data it is possible to extract the kinetically relevant pK_a values for the three complexes, *i.e.* pK_{a1} = 7.14, 7.90 or 8.43, and pK_{a2} = 9.21, 10.21 or 10.69 for $[Zn_2(L1)(CH_3COO)_2](PF_6)$, $[Zn_2(L2)(CH_3COO)_2](BPh_4)$ or $[Zn_2(L3)(CH_3COO)_2](BPh_4)$, respectively.

For each of the three Zn complexes the dependence of the reaction rate on the substrate (BDNPP) concentration was measured at the respective pH optima (*i.e.* pH 8, 9.0 and 9.5; Fig. 2b). The data were fitted using non-linear least square analysis to provide an estimate for the k_{cat} value and Michaelis constant (K_m): k_{cat} = 5.44(0.11) × 10^{-5} s^{-1}, 2.60(0.87) × 10^{-4} s^{-1} or 1.53(0.27) × 10^{-4} s^{-1}, and K_m = 5.13(0.92) mM, 5.49(1.51) mM or 2.14(0.50) mM for $[Zn_2(L1)(CH_3COO)_2](PF_6)$, $[Zn_2(L2)(CH_3COO)_2](BPh_4)$ or $[Zn_2(L3)(CH_3COO)_2](BPh_4)$, respectively. In each case the k_{cat} value shows an acceleration of the reaction rate of at least ~10^3 fold over the uncatalyzed hydrolysis of BDNPP (k_{uncat} = 3.88 × 10^{-7} s^{-1}) [82].

The $[Mg_2(L2)(CH_3COO)_2](BPh_4)$ complex displayed very low activity over the entire pH range and was thus not further investigated. A DFT study of the hydrolysis mechanisms of the phosphomonoester *p*-nitrophenylphosphate catalyzed by unsymmetrical dinuclear $Zn(II)_2$ and $Mg(II)_2$ complexes [41] concluded that, based on its hard base properties, Mg(II) ion should be able to substitute for other divalent ions in dinuclear phosphatases [41]. However, as demonstrated above, and at least for the systems reported in this work, Mg(II) is not capable of effectively replacing Zn(II) to promote the hydrolysis of substrates such as the activated phosphoester BDNPP.

The pH rate profiles for the zinc complexes are consistent with the existence of two protonation equilibria relevant for the reaction; for each complex the deprotonation associated with pK_{a1} leads to an activation of the reaction, whereas the deprotonation associated with pK_{a2} has the opposite effect. The magnitude of the pK_{a1} values are consistent with their assignment to either a zinc(II)-bound pendant alcohol or a zinc(II)-bound water molecule [1]. Both are potential nucleophiles in these complexes and both have been suggested previously to be active in such systems [1,31]. Studies have suggested that a zinc(II)-

Please cite this article as: J.J. Brown, et al., Investigation of the identity of the nucleophile initiating the hydrolysis of phosphate esters catalyzed by dinuclear mimics of me..., J. Inorg. Biochem. (2016), http://dx.doi.org/10.1016/j.jinorgbio.2016.02.008

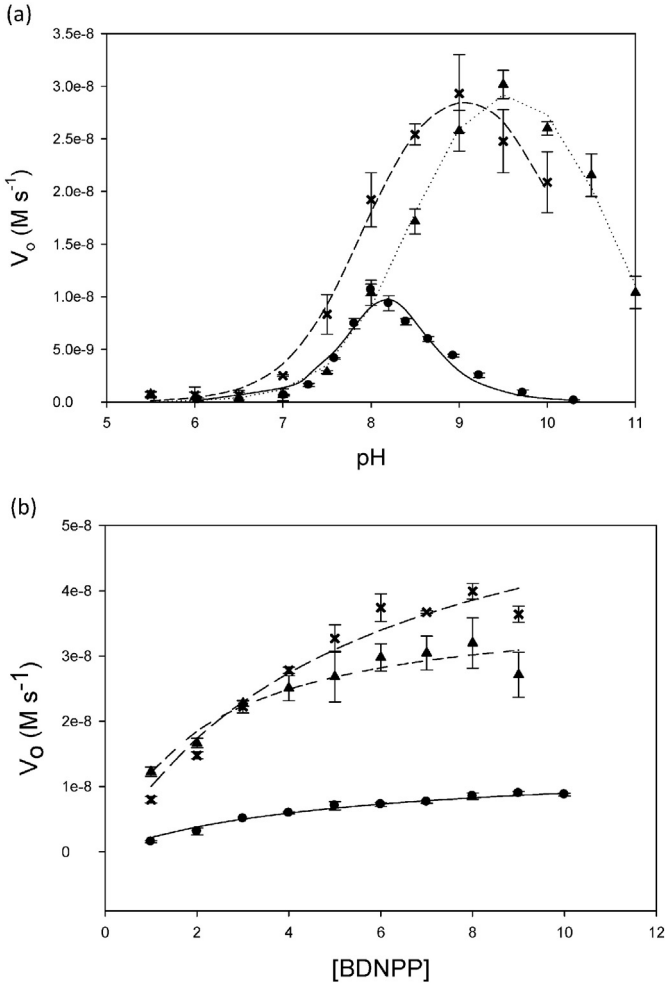

Fig. 2. (a) Plot of pH dependence of initial rate of BDNPP hydrolysis (5 mM) by $[Zn_2(L1)(CH_3COO)_2](PF_6)$ (●), $[Zn_2(L2)(CH_3COO)_2](BPh_4)$ (x), and $[Zn_2(L3)(CH_3COO)_2](BPh_4)$ (♦): the fit to the data using Eq. (1) is shown as the solid line. (b) Plot of substrate dependence of initial rate of BDNPP hydrolysis (5 mM) by $[Zn_2(L1)(CH_3COO)_2](PF_6)$ (●) (pH 8), $[Zn_2(L2)(CH_3COO)_2](BPh_4)$ (x) (pH 9), $[Zn_2(L3)(CH_3COO)_2](BPh_4)$ (♦) (pH 9.5); the fit to the data using the Michaelis–Menten equation is shown as the solid lines.

coordinated alcohol has a lower pK_a than a zinc(II)-coordinated water [30,31,83–85], however the differences may not be significant and the unambiguous identification of the relevant nucleophile is frequently dependent on additional data such as those from labeling studies with $H_2O^{16/18}$ [1]. However, even then the possibility of a mechanism involving both a Zn–OH moiety and a bound alkoxide in a two-step reaction may not be discounted [1]. In the case of $[Zn_2(L1)(CH_3COO)_2](PF_6)$ the assignment of the nucleophile (*i.e.* pK_{a1}) is unambiguous in that the molecule does not contain a coordinated alkoxide (Chart 1) and the ether donors are not nucleophilic; hence, here pK_{a1} is assigned to a Zn–OH_2 moiety. For the other two complexes, $[Zn_2(L2)(CH_3COO)_2](BPh_4)$ and $[Zn_2(L3)(CH_3COO)_2](BPh_4)$, the situation is less straightforward. The catalytic parameters of all three complexes are similar to those of various examples of di-Zn(II) complexes of this type [25,78]. For $[Zn_2(L1)(CH_3COO)_2](PF_6)$ a coordinated hydroxido ligand can be proposed as the active nucleophile; as for the other complexes $[Zn_2(L2)(CH_3COO)_2](BPh_4)$ has a symmetric donor set and alkoxide donors, and $[Zn_2(L3)(CH_3COO)_2](BPh_4)$ is an example of a system with an asymmetric donor set and these are predicted to be more realistic models for the enzyme systems [23]. In order to understand more of the potential mechanistic pathways for the reactions of these complexes computational studies were undertaken.

3.4. Computational modeling

Density functional theory (DFT) calculations were performed to explore the roles of coordinated hydroxide and alkoxide nucleophiles in the mechanism of phosphorolysis; specifically, the calculations focused on the di-zinc complex of L2 (Chart 1), in which either a metal-bound water molecule or one of the alcohol ligands could give rise to the catalytic nucleophile. bis(*para*-Nitrophenyl)phosphate (BNPP) was used as the model substrate. The computations were performed at the M06/6-31G(d,p)-LANL2DZ//B3LYP/6-31G(d)-LANL2DZ level of theory [50–53,55], simulating an aqueous medium with the SMD implicit solvent model [54]. Density functional theory calculations have previously been used to study phosphate and amide hydrolysis by related dizinc complexes [21,40,41,85–89].

Generation of the catalytically active complex from $[Zn_2(L2)(CH_3COO)_2]^+$ is thought to require the initial dissociation of the acetate ligands [27,90]. One or more of the coordination sites made available by the loss of these acetate groups is likely to be occupied by water molecules, but their exact number is not known (and may also vary in different systems). Therefore, a range of possible pathways were modeled, involving zero, one or two water ligands, coordinated in either a monodentate or metal-bridging mode. Different binding modes for the phosphate ester substrate (*i.e.* mono-, bi- or tridentate) were also explored, with either a coordinated hydroxide or alkoxide acting as the catalytic nucleophile.

Scheme 1 shows the lowest-energy reaction mechanisms that were identified for hydroxide (Path A) and alkoxide (Path B) nucleophiles. Both pathways originate from the same starting complex (**1**), which contains one water molecule bound to zinc. The water is deprotonated to form the catalytic nucleophile in the hydroxide-mediated pathway (Path A), and is a spectator in the alkoxide-mediated pathway (Path B). The kinetically relevant pK_{a1} for this complex (7.91) is consistent with deprotonation of either a metal-bound water or alkoxide and it is likely that both of the monodeprotonated species, $\mathbf{1a}^-$ and $\mathbf{1b}^-$, may be capable of formation at pH 9, the conditions of the experiment. The calculations suggest that in Path A, the nucleophilic hydroxide prefers to be bound to a single zinc centre only, rather than bridging between the two zinc ions. Geometry optimizations commencing with a bridging hydroxide converged to a monodentate complex. The geometries of the transition states for nucleophilic attack on BNPP by the coordinated hydroxide (TSA) or alkoxide (TSB) are shown in Fig. 3.

Importantly, the metal ion harboring the nucleophile is six-coordinate, while the other one has five ligands only. In both hydrolysis pathways, the nucleophile prefers to occupy a coordination site in *cis* position relative to the nitrogen and the phenolate oxygen ligands. Attack on BNPP by the hydroxide nucleophile (TSA) is computed to have an activation barrier $\Delta G^{\ddagger}$ of 23.9 kcal/mol, while attack by the alkoxide nucleophile (TSB) has a barrier of 34.5 kcal/mol. These $\Delta G^{\ddagger}$ values are computed with respect to the most stable form of the monodeprotonated reactant complex $\mathbf{1}^-$ (see the Supporting Information). The immediate products of hydroxide and alkoxide attack are phosphoranes **2** and **3**, respectively. These phosphoranes are predicted to occupy shallow energy wells, where the barrier for the loss of one of the nitrophenolate leaving groups is small or nonexistent. The phosphorane intermediate **2** in the hydroxide-mediated pathway (Path A) loses one nitrophenolate moiety to form **4**, which is a complex of $Zn_2(L2)$ with the product, *i.e.* $(p\text{-}NO_2C_6H_4O)P(OH)O_2^-$. Ligand exchange with BNPP and water is proposed to complete the catalytic cycle. In the alkoxido-mediated pathway (Path B), after the loss of the nitrophenolate leaving group from phosphorane **3** the phosphorus remains covalently bound to L2 (see **5**). Completion of the catalytic cycle requires hydrolysis of the covalent alkoxido–phosphate bond. The mechanism of this step is unknown and requires a second nucleophile. While the identity of this nucleophile remains obscure, the 10.6 kcal/mol difference in activation barriers between TSA and TSB indicates that the alkoxide-mediated pathway (Path B) is highly

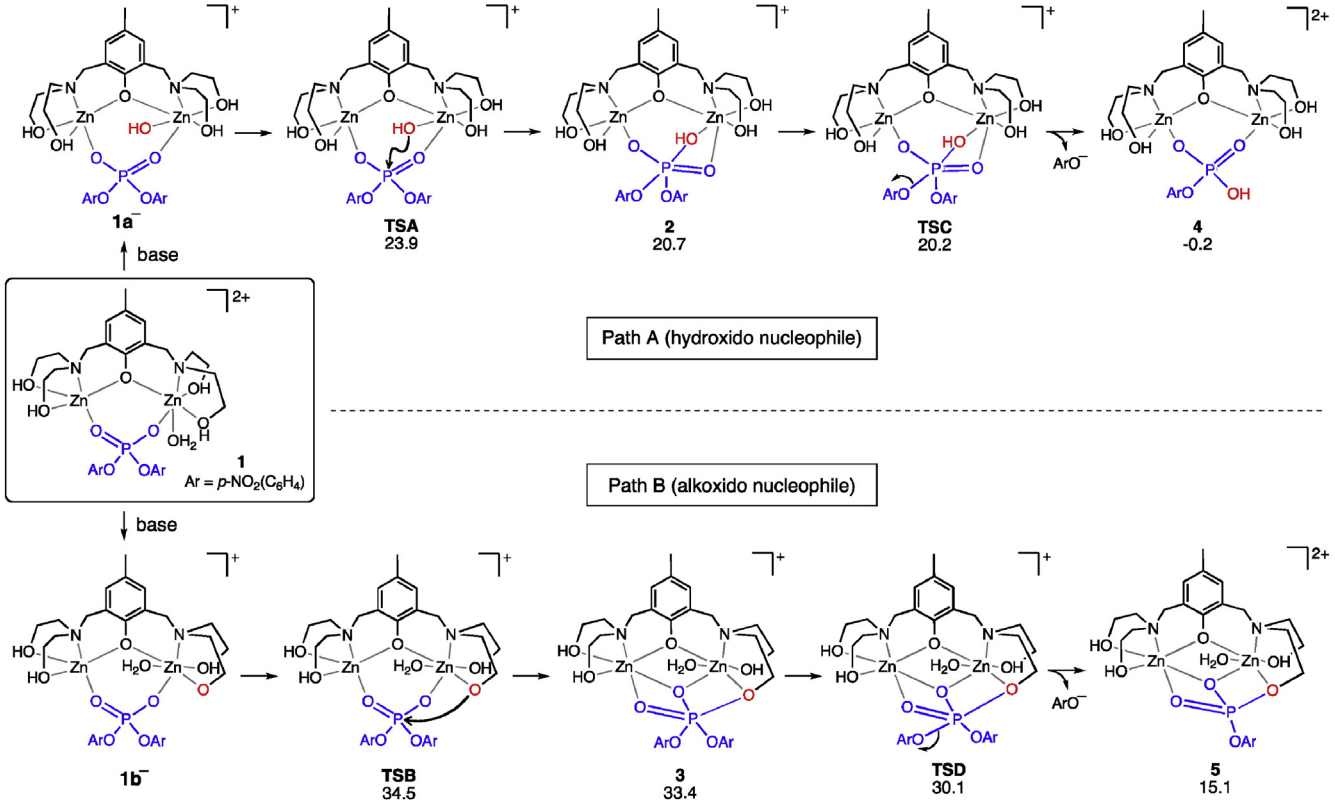

Scheme 1. Computed reaction mechanisms for hydrolysis of BNPP by the dizinc complex of L2 involving either a coordinated hydroxide nucleophile (Path A) or a coordinated alkoxide nucleophile (Path B). Gibbs free energies in water computed with M06/6-31G(d,p)-LANL2DZ//B3LYP/6-31G(d)-LANL2DZ are shown (kcal/mol).

unfavorable and is thus unlikely to play any significant role in phosphate ester hydrolysis at 25 °C.

The different barrier heights for hydroxido- and alkoxido-mediated attacks reflect the different degrees of structural reorganization that the $Zn_2(L2)$ unit undergoes when forming the respective transition states TSA and TSB. This is illustrated by the top-down views of the precatalyst and the transition states, shown in Fig. 3(b). In the favored TSA, the $Zn_2(L2)$ unit has a similar conformation to that in precatalyst $[Zn_2(L2)(CH_3COO)_2](BPh_4)$. The phosphate is bound in such a way that two of its oxygen atoms are positioned, approximately, in the same coordination sites formerly occupied by the acetate groups. By contrast, in the alkoxido-mediated pathway, significant reorganization of the $Zn_2(L2)$ core occurs. One of the phosphate oxygen atoms in TSB is located underneath the phenolate group, where it binds to both metal centers. To accommodate this bridging interaction, the $Zn_2(L2)$ unit needs to undergo significant distortions. The structural reorganization is perhaps most evident in the angle between the Zn–Zn axis and the plane of the central phenolate ring (Fig. 3(b)); this angle is about 45° in both $[Zn_2(L2)(CH_3COO)_2](BPh_4)$ and in TSA, but has twisted to 20° in TSB. The structural reorganization of the Zn_2L2 unit in TSB induces strain within the L2 ligand and distortion of the zinc coordination spheres, which together represent the main reason for the high energy of TSB relative to TSA.

The calculations therefore reveal the important role of ligand structural rigidity. A related computational study revealing the influence of catalyst flexibility on the rates and mechanisms of phosphodiester hydrolysis by a di-zinc(II) complex of bismacrocyclic ligand II (Chart 1) was recently reported by Maxwell, Mosey, and Brown [91]. The mode of substrate binding and hydrolysis computed for the di-zinc(II) complex of L2 (TSA) resembles the mechanism recently proposed by Zhao et al. for the di-zinc(II) complex of macrocyclic oxyimine/phenolate ligand III (Chart 1) [41,89]. In that case, no alcohol donor was present but the binding mode of the phosphate between the metal centers in the transition state was the same as in TSA. DFT calculations predicted that for the macrocyclic complex, direct attack by a coordinated hydroxide was preferred relative to an alternative mechanism where the Zn–OH group deprotonated a nearby water molecule to generate the active nucleophile.

The calculated barrier ($\Delta G^{\ddagger}$) of 23.9 kcal/mol for hydroxide-mediated BNPP hydrolysis *via* TSA corresponds to a k_{cat} of 2×10^{-5} s^{-1}, which is in good agreement with the experimental k_{cat} of 2.60×10^{-4} s^{-1} for the hydrolysis of the more reactive substrate BDNPP (*vide supra*). The predicted lack of involvement of any alkoxide-mediated pathway agrees well with the experimental k_{cat} values for the di-Zn(II) complexes of L1, L2, and L3, which vary by a factor of only five. The similar k_{cat} values are consistent with a common catalytic mechanism, where the small differences in rates for the complexes of L1–L3 would reflect small differences in the nucleophilicity of the coordinated hydroxide in each complex, rather than a role for alkoxido-mediated pathways in the L2 and L3 complexes.

4. Conclusions

The synthesis and characterization of the di-zinc(II) complexes of the ligands 2,6-bis((bis(2-methoxyethyl)amino)methyl)-4-methylphenol (HL1), 2,6-bis(bis(hydroxyethyl)aminomethyl)-4-methylphenol (HL2), and 2,6-bis((hydroxyethyl)(methoxyethyl)-aminomethyl)-4-methylphenol (HL3) has been investigated. The ligands differ in their donor types with HL1 having ether donors, HL2 alkoxido donors and HL3, being an asymmetric ligand, possessing both ether and alkoxido donors. The goal was to investigate the role of the potential nucleophiles in the hydrolysis reaction with the phosphodiester substrate BDNPP. In addition the di-Mg(II) complex of ligand HL2 was prepared in order to examine the potential for Mg(II) to replace Zn(II) in these biomimetic systems. The three di-zinc(II) complexes were found to display very similar pK_a values irrespective of the

Please cite this article as: J.J. Brown, et al., Investigation of the identity of the nucleophile initiating the hydrolysis of phosphate esters catalyzed by dinuclear mimics of me..., J. Inorg. Biochem. (2016), http://dx.doi.org/10.1016/j.jinorgbio.2016.02.008

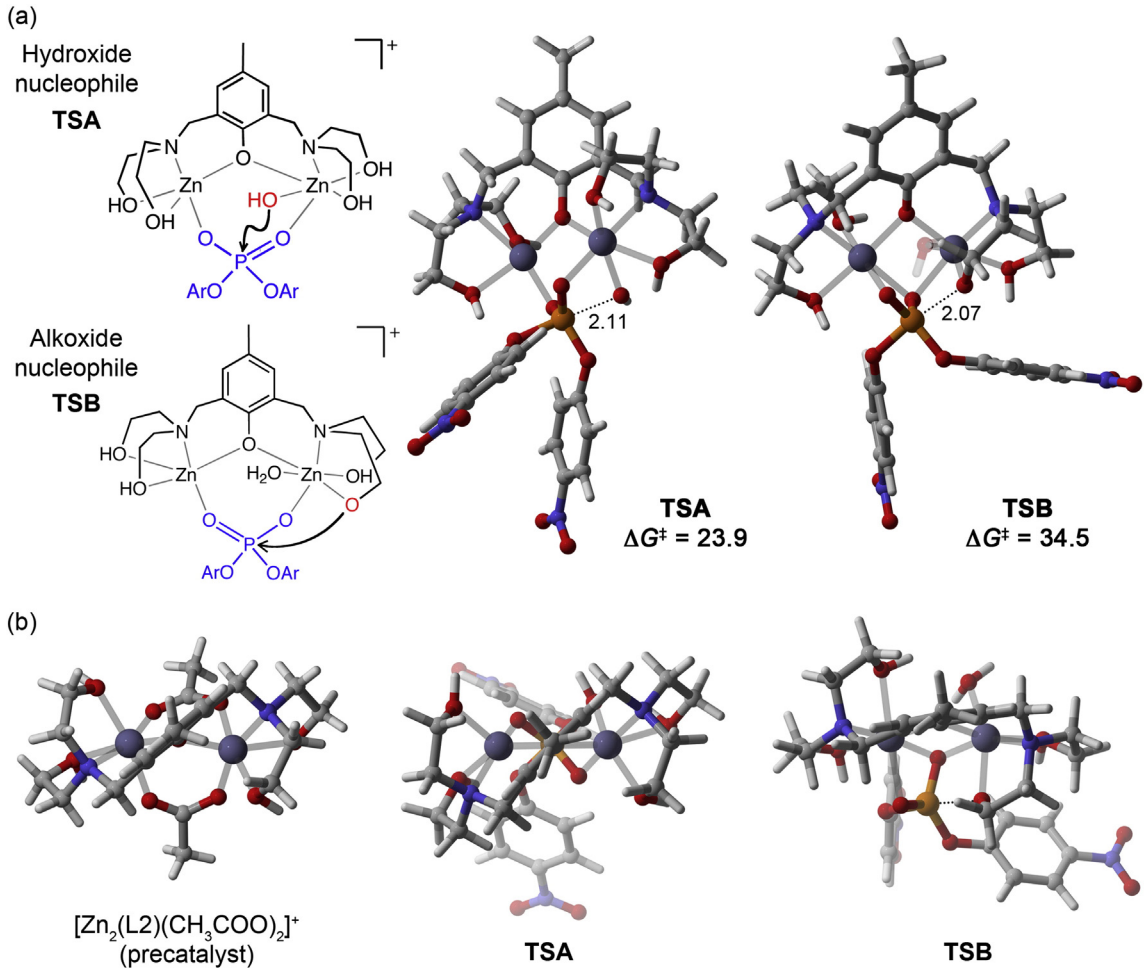

Fig. 3. (a) Transition states for hydrolysis of BNPP by the dizinc complex of L2 in water, computed at the M06/6-31G(d,p)-LANL2DZ//B3LYP/6-31G(d)-LANL2DZ level of theory (bond distances in Å, $\Delta G^{\ddagger}$ in kcal/mol). (b) Top-down views showing the conformation of the $Zn_2(L2)$ unit in TSA and TSB as compared with the X-ray structure of $[Zn_2(L2)(CH_3COO)_2](BPh_4)$.

presence of potential hydroxido or alkoxido nucleophiles; Computational methods were used in an attempt to discriminate between the mechanistic pathways possible for these systems. The DFT calculations indicate that an alkoxido-mediated pathway in the complexes formed with ligands L2 or L3 is unlikely, because it induces significant distortion of the $Zn_2(L)$ unit; a direct attack by a coordinated hydroxide is preferred in each of the three systems studied here. Interestingly, and in contrast to a previous theoretical study, Mg(II) was not able to reconstitute significant catalytic activity.

Acknowledgments

This work is financially supported by the Australian Research Council, Discovery Projects Scheme (DP120104263 and DP150104358). G.S. and E.H.K. also acknowledge the receipt of ARC Future Fellowships (FT120100694 to G.S. and FT120100632 to E.H.K.). This work was supported by computational resources provided by the Australian Government through the National Computational Infrastructure National Facility under the National Computational Merit Allocation Scheme, and by the University of Queensland Research Computing Centre. We are grateful to Prof. Paul Bernhardt (UQ) for his help with the crystal structure analysis.

Appendix A. Supplementary data

Supplementary data to this article can be found online at http://dx.doi.org/10.1016/j.jinorgbio.2016.02.008.

References

[1] L.J. Daumann, K.E. Dalle, G. Schenk, R.P. McGeary, P.V. Bernhardt, D.L. Ollis, L.R. Gahan, Dalton Trans. 41 (2012) 1695–1708.
[2] F. Meyer, P. Rutsch, Chem. Commun. (1998) 1037–1038.
[3] H. Daiyasu, K. Osaka, Y. Ishino, H. Toh, FEBS Lett. 503 (2001) 1–6.
[4] F. Meyer, Eur. J. Inorg. Chem. (2006) 3789–3800.
[5] D.L. Tierney, G. Schenk, Biophys. J. 107 (2014) 1263–1272.
[6] B. Bauer-Siebenlist, F. Meyer, E. Farkas, D. Vidovic, S. Dechert, Chem. Eur. J. 11 (2005) 4349–4360.
[7] C. Bazzicalupi, A. Bencini, C. Bonaccini, C. Giorgi, P. Gratteri, S. Moro, M. Palumbo, A. Simionato, J. Sgrignani, C. Sissi, B. Valtancoli, Inorg. Chem. 47 (2008) 5473–5484.
[8] N.J. Cosper, D.L. Bienvenue, J.E. Shokes, D.M. Gilner, T. Tsukamoto, R.A. Scott, R.C. Holz, J. Am. Chem. Soc. 125 (2003) 14654–14655.
[9] M. Egertova, G.M. Simon, B.F. Cravatt, M.R. Elphick, J. Comp. Neurol. 506 (2007) 604–615.
[10] C. He, S.J. Lippard, J. Am. Chem. Soc. 122 (2000) 184–185.
[11] N.V. Kaminskaia, C. He, S.J. Lippard, Inorg. Chem. 39 (2000) 3365–3373.
[12] B. Malfroy, H. Kado-Fong, C. Gros, B. Giros, J.C. Schwartz, R. Hellmiss, Biochem. Biophys. Res. Commun. 161 (1989) 236–241.
[13] A.L. Stamp, P. Owen, K. El Omari, C.E. Nichols, M. Lockyer, H.K. Lamb, I.G. Charles, A.R. Hawkins, D.K. Stammers, Protein Sci. 19 (2010) 1897–1905.
[14] S. Viars, J. Valentine, M. Hernick, Biomolecules 4 (2014) 527–545 (519 pp.).
[15] M.L. Zastrow, A.F.A. Peacock, J.A. Stuckey, V.L. Pecoraro, Nat. Chem. 4 (2012) 118–123.
[16] Z. Zhang, J. Liu, Q. Luo, J. Zhang, J. Xu, X.X. Zhu, Org. Biomol. Chem. 9 (2011) 8220–8223.
[17] M. Zhao, L. Zhang, H.-Y. Chen, H.-L. Wang, L.-N. Ji, Z.-W. Mao, Chem. Commun. 46 (2010) 6497–6499.
[18] Y.-H. Zhou, H. Fu, W.-X. Zhao, M.-L. Tong, C.-Y. Su, H. Sun, L.-N. Ji, Z.-W. Mao, Chem. Eur. J. 13 (2007) 2402–2409.
[19] Y.-H. Zhou, M. Zhao, H. Sun, Z.-W. Mao, L.-N. Ji, J. Mol. Catal. A Chem. 308 (2009) 61–67.
[20] H. Sakiyama, Y. Igarashi, Y. Nakayama, M.J. Hossain, K. Unoura, Y. Nishida, Inorg. Chim. Acta 351 (2003) 256–260.

[21] N. Guo, J.-Y. Zhong, S.-L. Chen, J.-Q. Liu, Q. Min, R.-X. Shi, Chem. Phys. 457 (2015) 70–77.
[22] M.J. Hossain, A. Wada, Y. Igarashi, K.-i. Aimono, K. Suzuki, K. Tone, H. Sakiyama, Int. J. Inorg. Chem. (2011) 395418 (395414 pp.).
[23] L.J. Daumann, L. Marty, G. Schenk, L.R. Gahan, Dalton Trans. 42 (2013) 9574–9584.
[24] L.J. Daumann, P. Comba, J.A. Larrabee, G. Schenk, R. Stranger, G. Cavigliasso, L.R. Gahan, Inorg. Chem. 52 (2013) 2029–2043.
[25] L.J. Daumann, G. Schenk, D.L. Ollis, L.R. Gahan, Dalton Trans. 43 (2014) 910–928.
[26] L.J. Daumann, L.R. Gahan, P. Comba, G. Schenk, Inorg. Chem. 51 (2012) 7669–7681.
[27] N. Mitić, S.J. Smith, A. Neves, L.W. Guddat, L.R. Gahan, G. Schenk, Chem. Rev. 106 (2006) 3338–3363.
[28] R.R. Buchholz, M.E. Etienne, A. Dorgelo, R.E. Mirams, S.J. Smith, S.Y. Chow, L.R. Hanton, G.B. Jameson, G. Schenk, L.R. Gahan, Dalton Trans. (2008) 6045–6054.
[29] G. Schenk, N. Mitić, L.R. Gahan, D.L. Ollis, R.P. McGeary, L.W. Guddat, Acc. Chem. Res. 45 (2013) 1593–1603.
[30] J. Chen, X. Wang, Y. Zhu, J. Lin, X. Yang, Y. Li, Y. Lu, Z. Guo, Inorg. Chem. 44 (2005) 3422–3430.
[31] C. Bazzicalupi, A. Bencini, E. Berni, A. Bianchi, V. Fedi, V. Fusi, C. Giorgi, P. Paoletti, B. Valtancoli, Inorg. Chem. 38 (1999) 4115–4122.
[32] H. Sakiyama, Inorg. Chim. Acta 360 (2007) 715–716.
[33] H. Sakiyama, R. Ito, H. Kumagai, K. Inoue, M. Sakamoto, Y. Nishida, M. Yamasaki, Eur. J. Inorg. Chem. (2001) 2705.
[34] H. Sakiyama, R. Ito, H. Kumagai, K. Inoue, M. Sakamoto, Y. Nishida, M. Yamasaki, Eur. J. Inorg. Chem. (2001) 2027–2032.
[35] H. Sakiyama, R. Mochizuki, A. Sugawara, M. Sakamoto, Y. Nishida, M. Yamasaki, J. Chem. Soc. Dalton Trans. (1999) 997–1000.
[36] H. Sakiyama, A. Sugawara, M. Sakamoto, K. Unoura, K. Inoue, M. Yamasaki, Inorg. Chim. Acta 310 (2000) 163–168.
[37] H. Sakiyama, T. Suzuki, K. Ono, R. Ito, Y. Watanabe, M. Yamasaki, M. Mikuriya, Inorg. Chim. Acta 358 (2005) 1897–1903.
[38] H. Sakiyama, M. Yamasaki, T. Suzuki, Y. Watanabe, R. Ito, A. Ohnishi, Y. Nishida, Inorg. Chem. Commun. 9 (2006) 18–20.
[39] R. Sanyal, S.K. Dash, S. Das, S. Chattopadhyay, S. Roy, D. Das, J. Biol. Inorg. Chem. 19 (2014) 1099–1111.
[40] R. Sanyal, A. Guha, T. Ghosh, T.K. Mondal, E. Zangrando, D. Das, Inorg. Chem. 53 (2014) 85–96.
[41] X. Zhang, Y. Zhu, X. Zheng, D.L. Phillips, C. Zhao, Inorg. Chem. 53 (2014) 3354–3361.
[42] M.M.E. de Backer, S. McSweeney, P.F. Lindley, E. Hough, Acta Crystallogr. Sect. D Biol. Crystallogr. D60 (2004) 1555–1561.
[43] P. Gettins, J.E. Coleman, Fed. Proc. 41 (1982) 2966–2973.
[44] G.M. Sheldrick, SHELXL97: Program for the refinement of crystal structures, University of Gottingen, Germany, 1997.
[45] L.J. Farrugia, J. Appl. Crystallogr. 32 (1999) 837–838.
[46] R.T. Paine, Y.-C. Tan, X.-M. Gan, Inorg. Chem. 40 (2001) 7009–7013.
[47] N.V. Kaminskaia, B. Spingler, S.J. Lippard, J. Am. Chem. Soc. 122 (2000) 6411–6422.
[48] L.J. Daumann, J.A. Larrabee, P. Comba, G. Schenk, L.R. Gahan, Eur. J. Inorg. Chem. (2013) 3082–3089.
[49] M.J. Frisch, G.W. Trucks, H.B. Schlegel, G.E. Scuseria, M.A. Robb, J.R. Cheeseman, G. Scalmani, V. Barone, B. Mennucci, G.A. Petersson, H. Nakatsuji, M. Caricato, X. Li, H.P. Hratchian, A.F. Izmaylov, J. Bloino, G. Zheng, J.L. Sonnenberg, M. Hada, M. Ehara, K. Toyota, R. Fukuda, J. Hasegawa, M. Ishida, T. Nakajima, Y. Honda, O. Kitao, H. Nakai, T. Vreven, J.A. Montgomery Jr., J.E. Peralta, F. Ogliaro, M. Bearpark, J.J. Heyd, E. Brothers, K.N. Kudin, V.N. Staroverov, R. Kobayashi, J. Normand, K. Raghavachari, A. Rendell, J.C. Burant, S.S. Iyengar, J. Tomasi, M. Cossi, N. Rega, J.M. Millam, M. Klene, J.E. Knox, J.B. Cross, V. Bakken, C. Adamo, J. Jaramillo, R. Gomperts, R.E. Stratmann, O. Yazyev, A.J. Austin, R. Cammi, C. Pomelli, J.W. Ochterski, R.L. Martin, K. Morokuma, V.G. Zakrzewski, G.A. Voth, P. Salvador, J.J. Dannenberg, S. Dapprich, A.D. Daniels, Ö Farkas, J.B. Foresman, J.V. Ortiz, J. Cioslowski, D.J. Fox, Gaussian 09, Revision D.01, Gaussian, Inc., Wallingford CT, 2009.
[50] C. Lee, W. Yang, R.G. Parr, Phys. Rev. B Condens. Matter 37 (1988) 785–789.
[51] A.D. Becke, J. Chem. Phys. 98 (1993) 1372–1377.
[52] A.D. Becke, J. Chem. Phys. 98 (1993) 5648–5652.
[53] P.J. Stephens, F.J. Devlin, C.F. Chabalowski, M.J. Frisch, J. Phys. Chem. 98 (1994) 11623–11627.
[54] A.V. Marenich, C.J. Cramer, D.G. Truhlar, J. Phys. Chem. B 113 (2009) 6378–6396.
[55] Y. Zhao, D.G. Truhlar, Theor. Chem. Accounts 120 (2008) 215–241.
[56] K.E. Dalle, L.J. Daumann, G. Schenk, R.P. McGeary, L.R. Hanton, L.R. Gahan, Polyhedron 52 (2013) 1336–1343.
[57] P.K. Saini, C. Romain, Y. Zhu, C.K. Williams, Polym. Chem. 5 (2014) 6068–6075.
[58] P.K. Saini, C. Romain, C.K. Williams, Chem. Commun. 50 (2014) 4164–4167.
[59] W. Yi, H. Ma, Dalton Trans. 43 (2014) 5200–5210.
[60] W. Yi, H. Ma, Inorg. Chem. 52 (2013) 11821–11835.
[61] M.R. Kember, C.K. Williams, J. Am. Chem. Soc. 134 (2012) 15676–15679.
[62] C.-Y. Li, C.-R. Wu, Y.-C. Liu, B.-T. Ko, Chem. Commun. 48 (2012) 9628–9630.
[63] S. Dutta, P. Biswas, U. Florke, K. Nag, Inorg. Chem. 49 (2010) 7382–7400.
[64] V. Chandrasekhar, B. Murugesapandian, T. Senapati, P. Bag, M.D. Pandey, S.K. Maurya, D. Goswami, Inorg. Chem. 49 (2010) 4008–4016.
[65] A.C. Raimondi, D.J. Evans, T. Hasegawa, S.M. Drechsel, F.S. Nunes, Spectrochim. Acta A 67A (2007) 145–149.
[66] D. Zhang, H. Kawaguchi, Organometallics 25 (2006) 5506–5509.
[67] A.C. Raimondi, V.R. de Souza, H.E. Toma, D.J. Evans, T. Hasegawa, F.S. Nunes, Spectrochim. Acta A 61A (2005) 1929–1932.
[68] V. Chandrasekhar, R. Azhakar, J.F. Bickley, A. Steiner, Chem. Commun. (2005) 459–461.
[69] A.C. Raimondi, V.R. de Souza, H.E. Toma, A.S. Mangrich, T. Hasegawa, F.S. Nunes, Polyhedron 23 (2004) 2069–2074.
[70] F. Gao, B.H. Meng, Y.B. Wei, Acta Crystallogr. Sect. C Cryst. Struct. Commun. C60 (2004) m360–m362.
[71] A.C. Raimondi, P.B. Hitchcock, G.J. Leigh, F.S. Nunes, J. Chem. Crystallogr. 34 (2004) 83–87.
[72] R.L. Dutta, R.K. Ray, J. Indian Chem. Soc. 60 (1983) 185–186.
[73] E. Lambert, B. Chabut, S. Chardon-Noblat, A. Deronzier, G. Chottard, A. Bousseksou, J.-P. Tuchagues, J. Laugier, M. Bardet, J.-M. Latour, J. Am. Chem. Soc. 119 (1997) 9424–9437.
[74] B. Das, H. Daver, A. Singh, R. Singh, M. Haukka, S. Demeshko, F. Meyer, G. Lisensky, M. Jarenmark, F. Himo, E. Nordlander, Eur. J. Inorg. Chem. (2014) 2204–2212.
[75] F.R. Xavier, A.J. Bortoluzzi, A. Neves, Chem. Biodivers. 9 (2012) 1794–1805.
[76] F.R. Xavier, A. Neves, A. Casellato, R.A. Peralta, A.J. Bortoluzzi, B. Szpoganicz, P.C. Severino, H. Terenzi, Z. Tomkowicz, S. Ostrovsky, W. Haase, A. Ozarowski, J. Krzystek, J. Telser, G. Schenk, L.R. Gahan, Inorg. Chem. 48 (2009) 7905–7921.
[77] F.R. Xavier, R.A. Peralta, A.J. Bortoluzzi, V. Drago, E.E. Castellano, W. Haase, Z. Tomkowicz, A. Neves, J. Inorg. Biochem. 105 (2011) 1740–1752.
[78] L.J. Daumann, Spectroscopic and Mechanistic Studies of Dinuclear Metallohydrolases and their Biomimetic Complexes, Springer International Publishing, Switzerland, 2014.
[79] S. Drueke, K. Wieghardt, B. Nuber, J. Weiss, H.P. Fleischhauer, S. Gehring, W. Haase, J. Am. Chem. Soc. 111 (1989) 8622–8631.
[80] M. Lanznaster, A. Neves, A.J. Bortoluzzi, B. Szpoganicz, E. Schwingel, Inorg. Chem. 41 (2002) 5641–5643.
[81] I.H. Segel, Enzyme Kinetics: Behavior and Analysis of Rapid Equilibrium and Steady State Enzyme Systems, Wiley-Interscience, New York, 1975.
[82] A. Greatti, M. Scarpellini, R.A. Peralta, A. Casellato, A.J. Bortoluzzi, F.R. Xavier, R. Jovito, M. Aires de Brito, B. Szpoganicz, Z. Tomkowicz, M. Rams, W. Haase, A. Neves, Inorg. Chem. 47 (2008) 1107–1119.
[83] E. Kimura, Y. Kodama, T. Koike, M. Shiro, J. Am. Chem. Soc. 117 (1995) 8304–8311.
[84] M. Livieri, F. Mancin, U. Tonellato, J. Chin, J. Chem. Soc. Chem. Commun. (2004) 2862–2863.
[85] J. Xia, Y.B. Shi, Y. Zhang, Q. Miao, W.X. Tang, Inorg. Chem. 42 (2003) 70–77.
[86] R. Sanyal, X. Zhang, P. Kundu, T. Chattopadhyay, C. Zhao, F.A. Mautner, D. Das, Inorg. Chem. 54 (2015) 2315–2324.
[87] H. Gao, Z. Ke, N.J. DeYonker, J. Wang, H. Xu, Z.-W. Mao, D.L. Phillips, C. Zhao, J. Am. Chem. Soc. 133 (2011) 2904–2915.
[88] S. Ishiyama, C. Kaneda, J. Shibayama, K. Suzuki, R. Yamaguchi, H. Sakiyama, J. Comput. Chem. Jpn. 13 (2014) 157–158.
[89] X. Zhang, X. Zheng, D.L. Phillips, C. Zhao, Dalton Trans. 43 (2014) 16289–16299.
[90] L.R. Gahan, S.J. Smith, A. Neves, G. Schenk, Eur. J. Inorg. Chem. (2009) 2745–2758.
[91] C.I. Maxwell, N.J. Mosey, R.S. Brown, J. Am. Chem. Soc. 135 (2013) 17209–17222.

Please cite this article as: J.J. Brown, et al., Investigation of the identity of the nucleophile initiating the hydrolysis of phosphate esters catalyzed by dinuclear mimics of me..., J. Inorg. Biochem. (2016), http://dx.doi.org/10.1016/j.jinorgbio.2016.02.008